Photoproduction of charmonium in a gluon-exchange model

B. Humpert
Stanford Linear Accelerator Center, Stanford University, Stanford, California 94305
(Received 29 August 1977)

A model describing photoproduction of a heavy-fermion pair which interacts by the exchange of gluons with the target is considered in the framework of the Cheng-Wu picture. Its characteristics are presented and it is applied to ψ_c and η_c photoproduction where the heavy quarks are assumed to be produced in the target's gluon potential. The angular distribution of orthocharmonium reveals a characteristic zero point at $\sqrt{-t} = 2m_c$ whereas the angular distribution of paracharmonium is flat. Arguments and estimates are given for the neglect of the gluon tree diagrams. The model applied to electromagnetic production of $(\tau^+\tau^-)$ shows that the inclusion of multiphoton exchanges enhances the cross sections by a factor 2–3.

I. INTRODUCTION

Photoproduction of a pair of bound heavy quarks ("charmonium") presents the attractive opportunity of studying several theoretical assumptions in strong-interaction dynamics. The interaction between the quarks, described by a non-Abelian gauge theory,[1,2] is at present subject to extensive phenomenological investigations.[3-5]

The binding of the quarks, attributed to the confinement mechanism,[6] allows the quarks to appear as quasifree objects at short distances. The large mass of the charmed quarks,[7] taken as a phenomenological fact, permits further study of the present understanding of strong-interaction dynamics. Apart from these conceptual theoretical questions one wonders why ψ photoproduction is suppressed in comparison to photoproduction of the light-quark vector mesons (ρ, ω, ϕ) and why its angular distribution is less peaked in the forward direction.[9]

Assuming a non-Abelian gauge-theory picture of strong-interaction dynamics,[1] we study the photoproduction of a heavy-quark pair which subsequently undergoes interaction with the conventional quarks via gluon exchange and eventually forms the bound state ψ $(c\bar{c})$. Measurable consequences of such a point of view have been found in an analysis of the spin dependence of ψ photoproduction.[10] Here, rather, we will concentrate on the angular distribution of this process and its parastate analog.[11] In the framework of quantum electrodynamics, such a picture has been studied extensively in the past by a number of authors.[12,13]

The main question we ask in this work is, "What implications has gluon exchange for the angular distribution?" The paper is organized as follows: In Sec. II we state our assumptions in the quantum-chromodynamics (QCD) framework[12] and introduce the basics of the infinite-momentum-frame calculus.[14] The general form of the scattering amplitude with the (fluctuation) wave functions of the photon and the quark bound state is discussed in Sec. III. Its structure is analyzed in Sec. IV, and it is cast into an easily calculable form which is used for the evaluation of our numerical results; these are presented and discussed in Sec. V. We have determined the cross sections for photoproduction of ψ_c and η_c as well as photoproduction of an unbound heavy-lepton pair $\tau^+\tau^-$.[15] The application of this model to photoproduction of quark pairs involves the neglect of gluon tree diagrams which, as we are able to show in Sec. VI, is well justified. Our results and conclusions are summarized in Sec. VII.

II. ASSUMPTIONS AND CALCULATION METHOD

Before going into the details of our work, we assemble the most important assumptions which stand behind our calculations. We first concentrate on QCD and then briefly introduce the infinite-momentum-frame technique as our calculation method.

The successes of non-Abelian gauge theories in unifying weak and electromagnetic interactions and the continuing attempts at a more general framework unifying weak, electromagnetic *and* strong interations[1] lead us to pursue the dynamical consequences of a field theory of the non-Abelian type in strong-interaction dynamics. It is generally agreed that this type of theory assembles the following ingredients: renormalizability, conservation of isospin, parity, etc., asymptotic freedom, no strongly interacting scalar fields, and color confinement. Explicit examples of such theories exist, but solid proof of color confinement is still missing. As a way out, one can argue that a perturbative treatment of such theories[16] is justified in regions where the running coupling constant is small.[17] In the following, we will adopt such a viewpoint by assuming that a

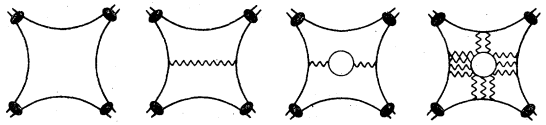

FIG. 1. Quark interaction in gluon theories.

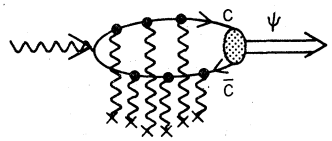

FIG. 2. Three-step picture of ψ $(c\bar{c})$ photoproduction in the gluon potential of the nucleon.

multigluon exchange lead to Pomeron-like characteristics. We consider the scattering process of a pair of charmed quarks in a scalar $1/r$ (long-range) potential. The bound-state nature of the quark pair is retained in the formal presentation of the model; however, it is ignored in the numerical evaluations since we are mostly concerned here with the consequences of gluon exchange. We first present the form of the scattering amplitude as given by Cheng and Wu.[18] Subsequently, we give the angular distribution of the ortho and para $c\bar{c}$ states; and, finally, we numerically determine the dependence of the scattering amplitude on the quark mass and study the influence and behavior of the multigluon-exchange contributions.

However, before embarking upon this program, and before deriving the form of the scattering amplitude, let us briefly introduce the basics of the infinite-momentum-frame calculus and with it our notation.

Owing to covariance and Lorentz invariance of the S matrix, the scattering processes can be viewed and described in any Lorentz frame. In particular, a Lorentz frame may be chosen where the form of the scattering amplitude reduces to a simpler expression and thus allows greater theoretical intuition, namely the infinite-momentum frame.[14]

The infinite-momentum-frame variables are defined by

$$(E, p_x, p_y, p_z) \to \left(\eta \equiv \frac{E+p_z}{\sqrt{2}}, p_x, p_y, H \equiv \frac{E-p_z}{\sqrt{2}}\right),$$
$$\vec{p} \equiv (p_x, p_y). \tag{2.1}$$

III. THE SCATTERING AMPLITUDE

Following the approach presented in Sec. II, the scattering process as described in Fig. 2 occurs in three steps: First, the incoming physical photon fluctuates into a system of freely moving constituents (c quarks), the partons in the DLY approach.[19] Second, each individual constituent undergoes instantaneous, elastic multiscattering processes in the gluon potential of the nucleon. There is no interaction between the quarks during this process. Finally, they interact to form the observed bound state. Within the gluon-exchange framework, this three-step picture is expected to be valid at high energies where the fluctuation lifetime is much larger than the time needed for the interaction with the external gluon potential.

This picture has been elegantly formulated by Bjorken, Kogut, and Soper,[14] using the infinite-momentum-frame calculus. The determination of the scattering amplitude requires consideration of the fluctuation wave functions due to the photon, the quark-pair bound state, and the amplitude describing the actual gluon-scattering process.

A. The photon fluctuation wave function

In the spirit of the parton approach, we assume that the initial photon state is expanded in a complete set of "bare" states, $\bar{\gamma}$—the bare photon and the partons—and write

$$|\gamma\rangle = |\bar{\gamma}\rangle + \int \sum d\Gamma_{12} M_{12}^{\gamma} |\bar{1}\rangle |\bar{2}\rangle + \cdots, \tag{3.1}$$

where

$$d\Gamma_{12} = \frac{d\vec{1}}{(2\pi)^3} \frac{d\eta^2}{2\eta_1} \frac{d\vec{1}_2}{(2\pi)^3} \frac{d\eta_2}{2\eta_2} \times (2\pi)^3 \delta(\eta - \eta_1 - \eta_2) \delta^2(\vec{L} - \vec{1}_1 - \vec{1}_2) \sqrt{2\eta_1 2\eta_2} \tag{3.2}$$

stands for the phase-space integration over the intermediate parton states which are characterized by their transverse momenta $\vec{1}_i$, longitudinal-momentum fractions η_i, spin s_i and all other quantum numbers. Since we are working on lowest-order electromagnetic interactions, only the two-parton intermediate state is relevant here. The photon fluctuation wave function is in principle a function of the total momentum $\vec{L} = \vec{1}_1 + \vec{1}_2$, $\eta = \eta_1 + \eta_2$, and also depends on the momentum components of the two intermediate partons; but it can easily be shown to depend only on the variable combinations

$$\vec{p} = \vec{1}_1 \cdot \beta_2 - \vec{1}_2 \cdot \beta_1, \quad \beta = \tfrac{1}{2}(\beta_1 - \beta_2) \tag{3.3}$$

because of Galilean invariance. Thus, to perform a Lorentz transformation is to change the variable $\vec{p}$ and β. The explicit form of the fluctuation wave functions in lowest-order QED have been determined in Ref. 14 using standard rules of the old-fashioned perturbation theory for time-ordered

Feynman diagrams with

$$\sqrt{2\eta_1 2\eta_2}\, M^\gamma = -e\,\frac{\bar{u}_1 \not{\epsilon} v_2}{H - H_1 - H_2}\,. \tag{3.4}$$

H and $H_{1,2}$ are the Hamiltonians of the bare photon and parton states in the infinite-momentum frame, and $\bar{u}_1$ and v_2 represent the spinors of the fermions. For explicit spin combinations we have

$$M^\gamma_{\pm 1,\pm\pm}(\vec{p},\beta) = e\,\frac{m}{m^2+\vec{p}^{\,2}}\sqrt{2}\,, \tag{3.5}$$

$$M^\gamma_{\pm 1,\pm\mp}(\vec{p},\beta) = \pm e(\tfrac{1}{2}\pm\beta)\,\frac{p_+}{m^2+\vec{p}^{\,2}}\sqrt{2}\,, \tag{3.6}$$

$$M^\gamma_{-1,\pm\mp}(\vec{p},\beta) = \pm e(\tfrac{1}{2}\mp\beta)\,\frac{p_-}{m^2+\vec{p}^{\,2}}\sqrt{2}\,, \tag{3.7}$$

$$M^\gamma_{\pm 1,\mp\mp}(\vec{p},\beta) = 0\,, \tag{3.8}$$

where $p_\pm = p_x \pm i p_y$.

B. Quark fluctuation

In a completely analogous manner, the final state $|\psi\rangle$ is expanded in parton-antiparton states (where here, however, no bare $|\bar{\psi}\rangle$ state is allowed since ψ is a bound state of a pair of quarks).

$$|\psi\rangle = \int \sum d\Gamma_{12} M^\psi_{12} |\,\vec{1}\,\rangle |\,\vec{2}\,\rangle + \cdots, \tag{3.9}$$

with the ψ fluctuation wave function $M^\psi_{12}(\vec{p}',\beta')$ being dependent on the momenta of the parton states $|\,\vec{\imath}\,\rangle$ and the total momentum $\vec{L}' = \vec{l}_1' + \vec{l}_2'$, $\eta' = \eta_1' + \eta_2'$ as defined in Eq. (2.2). Following Cheng and Wu,[18] we relate the bound-state fluctuation wave function $M^\psi(\vec{p},\beta')$ to the ordinary Schrödinger bound-state wave function $\phi_B(p)$ and describe the bound quark pair by

$$M^\psi(\vec{p}',\beta') = \sqrt{2M_B}\,\phi_B(\vec{p}', M_B\beta')\, C(\tfrac{1}{2},\lambda_1,\tfrac{1}{2},\lambda_2;s',\lambda')\,. \tag{3.10}$$

M_B is the mass of the bound-state system, s and λ' are its spin and helicity, and λ_1, λ_2 are the helicities of the partons. $C(\cdots;\cdots)$ stands for the Clebsch-Gordan coefficient. The Schrödinger wave function is normalized as usual:

$$\int \frac{d^3p}{(2\pi)^3}\,|\phi_B(\vec{p})|^2 = 1\,. \tag{3.11}$$

The above ansatz (3.10) is well justified as long as the quark masses are heavy and the binding energy is small. The factorization of the spin part from the space part in M^ψ is a good approximation if the internal motion of the partons can be neglected, and thus the appropriate Wigner rotation for spin projections onto the z axis may be neglected. If, for example, a $1/r$ potential between the quarks is assumed, the bound-state wave function reads[20]

$$\phi_B(\vec{p}) \propto \frac{(a_0^3)^{1/2}}{(1+a_0^2\vec{p}^{\,2})^2}\,, \quad a_0 \equiv \frac{2}{m\alpha_s}\,, \tag{3.12}$$

where a_0 is the radius of the bound state and $\alpha_s \equiv g_s^2/4\pi$ is the strong-coupling constant.

C. Scattering amplitude

We are now in a position to specify the scattering amplitude. We sandwich the scattering operator R (defined in $S = 1 + iR$) between the wave functions $|\psi\rangle$ and $|\gamma\rangle$ and obtain for the T matrix the well known result

$$T_{\lambda\lambda'}(\vec{u}) = \int \frac{d\vec{q}}{(2\pi)^2}\,[F_-(\vec{u}+\vec{q})F_+(\vec{u}-\vec{q}) - (2\pi)^4\delta^2(\vec{u}+\vec{q})\delta^2(\vec{u}-\vec{q})]\,J_{\lambda'\lambda}(\vec{u},\vec{q})\,, \tag{3.13}$$

where $(\vec{p}_i - \vec{p}_f) \equiv 2\vec{u}$, $\vec{p}_i$ ($\vec{p}_f$) represents the transverse momentum of the initial γ state (final ψ state), and $t = -(\vec{p}_i - \vec{p}_f)^2$. The "impact factor" $J_{\lambda'\lambda}$ contains all the information about the creation process and final-state binding of the constituent system through the fluctuation wave functions introduced above

$$J_{\lambda'\lambda}(\vec{u},\vec{q}) = \int_{-1/2}^{+1/2} d\beta \int_{-\infty}^{+\infty} \frac{d\vec{l}}{(2\pi)^2} \sum M^{\psi *}_{\lambda'}(\vec{l}+\vec{m},\beta)\, \times M^\gamma_\lambda(\vec{l}-\vec{m},\beta)\,, \tag{3.14}$$

where $\vec{m} = \frac{1}{2}\vec{q} - \beta\vec{u}$ and the sum extends over the fermion helicities which we have omitted. The differential cross section is

$$\frac{d\sigma}{d\Delta^2} = \frac{1}{(4\pi)^3}\,\overline{\sum}\,|T_{\lambda'\lambda}|^2\,. \tag{3.15}$$

The S-matrix amplitude describing the interaction of each constituent with the gluon potential is parametrized by the eikonal form

$$F_\pm(\vec{q}) = \int_{-\infty}^{+\infty} d\vec{b}\, e^{-\vec{q}\cdot\vec{b}}\, e^{\pm i\chi(\vec{b})}\,, \tag{3.16}$$

such that each constituent acquires an eikonal phase shift whereas their longitudinal momenta and helicities remain unchanged.

Let us for later purposes assume a Coulomb-type gluon potential

$$V(r) = \frac{g_s}{4\pi r}\,, \tag{3.17}$$

where g_s stands for the "strong charge". The phase shift $\chi(\vec{b})$ appearing in Eq. (3.16) is related to the potential $V(r)$ by

$$\chi(\vec{b}) = -\int_{-\infty}^{+\infty} dz\, g_s V(\vec{b},z)\,, \tag{3.18}$$

with the vector $\vec{b} \equiv (b_x, b_y)$ in impact-parameter space. The integration is easily performed once an auxiliary nonzero photon mass is introduced through a factor $e^{-\mu r}$ to prevent divergence of the integration. Then

$$\chi(\vec{b}) = -g_s^2 \int \frac{d\vec{q}}{(2\pi)^2} \frac{e^{i\vec{b}\cdot\vec{q}}}{\vec{q}^2+\mu^2} = -2\alpha_s K_0(\mu b) \xrightarrow[\mu\to 0]{} -2\alpha_s \left[\ln\left(\frac{\mu b}{2}\right)+\gamma\right], \quad (3.19)$$

and inserting this into Eq. (3.16) immediately gives the result

$$F_\pm(\vec{q}) = \mp i \frac{4\pi\alpha_s}{q^{2(1\mp i\alpha_s)}} e^{\mp i\Lambda(\mu,\alpha_s)}, \quad (3.20)$$

with the phase factor

$$\Lambda(\mu,\alpha_s) = 2[\alpha_s(\ln\mu+\gamma) + \arg\Gamma(1+i\alpha_s)], \quad (3.21)$$

depending logarithmically on the small photon mass μ. The formalism presented above [Eqs. (3.13)–(3.15)] has been derived in many different ways: for example, by summing the leading asymptotic behavior of Feynman diagrams, by the use of nonrelativistic multiparticle wave functions, by the use of relativistic eikonalization methods, and by the application of infinite-momentum-frame techniques.[12-14] We therefore do not consider it worthwhile to go into more details here. Instead, we are more concerned with the explicit evaluation of the scattering amplitude and the extraction of its dependence on the momentum transfer.

IV. EVALUATION OF THE AMPLITUDE

In the preceding section we have assembled all the necessary ingredients for the scattering amplitude and now are concerned with its explicit dependence on the momentum transfer $t \equiv -(\vec{p}_i - \vec{p}_f)^2$.

We start by considering the impact factor Eq. (3.14); its explicit form is

$$J_{\lambda\lambda'} = \int_{-1/2}^{+1/2} d\beta \int \frac{d\vec{l}}{(2\pi)^2} \sum M_\lambda^\gamma(\vec{l}-\vec{m},\beta)\sqrt{2M_B}\,\phi(\vec{l}+\vec{m},M_B\beta) C(\circ\cdots;s',\lambda'), \quad (4.1)$$

with $\vec{m}$ given in Eq. (3.14). λ and λ' are the spin of the photon and the final quark-antiquark bound state, and $\sum$ stands for the sum over the spins of the intermediate partons. One immediately realizes that the evaluation of the T matrix is very difficult in general and inelegant. We therefore ignore the influence of the bound state here and replace the bound-state wave function by a δ function which permits determination of $J_{\lambda\lambda'}$ in a simpler form:

$$J_{\lambda\lambda'} = \phi_0 \frac{2\pi}{\sqrt{2m}} \left[\sum_{\text{spins}} M_\lambda^\gamma C(\cdots s',\lambda')\right]. \quad (4.2)$$

By the explicit insertion of M_λ^γ and of the Clebsch-Gordan coefficient, (4.2) leads to

$$J_{0,\pm1} = -\phi_0 2\pi e \frac{q_+}{m^2+\vec{q}^2} \frac{1}{\sqrt{m}}, \quad (4.3)$$

$$J_{\pm1,\pm1} = +\phi_0 2\pi e \frac{m}{m^2+\vec{q}^2} \left(\frac{2}{m}\right)^{1/2}, \quad (4.4)$$

where

$$\phi_0 = \int \frac{d^3p}{(2\pi)^3} \phi(\vec{p}) \quad (4.5)$$

is the bound-state wave function at the origin.

We are now in a position to specify the T-matrix elements by inserting Eqs. (4.3) and (4.4) into Eq. (3.13). By defining the amplitudes for orthocharmonium and paracharmonium production

$$T^1 \equiv T_{\pm1,\pm1} = \sqrt{2}\,r R^1, \quad (4.6)$$

$$T_\pm^0 \equiv T_{0,\pm1} = r R^0, \quad (4.7)$$

with

$$r = \left(\frac{8\pi e}{\sqrt{m}}\right)\alpha_s^2\phi_0, \quad (4.8)$$

we have to determine the t dependence of the functions

$$R^1(t) = \int_{-\infty}^{+\infty} d\vec{q}\,\xi(\vec{u},\vec{q},\alpha_s)\left(\frac{1}{m^2+\vec{q}^2} - \frac{1}{m^2+\vec{u}^2}\right), \quad (4.9)$$

$$R^0(t) = \int_{-\infty}^{+\infty} d\vec{q}\,\xi(\vec{u},\vec{q},\alpha_s)\left(\frac{q_\pm}{m^2+\vec{q}^2}\right), \quad (4.10)$$

where

$$\xi(\vec{u},\vec{q},\alpha_s) = \frac{1}{(\vec{u}+\vec{q})^{2(1-i\alpha_s)}} \times \frac{1}{(\vec{u}-\vec{q})^{2(1+i\alpha_s)}} \quad (4.11)$$

is due to the product of form factors. In deriving Eq. (4.9) we have used the "regularized impact factor" and introduced the additional term $1/(m^2+\vec{q}^2)$ in order to weaken the divergence of the integrand at $\vec{q} = \pm\vec{u}$; this is allowed since the identity

$$\int d\vec{q}[F_-(\vec{q}+\vec{u})F_+(\vec{q}-\vec{u}) - (2\pi)^4\delta^2(\vec{u}+\vec{q})\delta^2(\vec{u}-\vec{q})]J(\vec{u},\vec{u})=0 \quad (4.12)$$

holds. In order to extract the t dependence of Eqs. (4.9) and (4.10) we use the generalized Feynman-parameter integrals,

$$\frac{1}{a^{1-\gamma}}\frac{1}{b^{1+\gamma}}=\frac{\sinh\pi\alpha_s}{\pi\alpha_s}\int_0^1 d\alpha\,\frac{\alpha^{-\gamma}(1-\alpha)^{\gamma}}{[\alpha a+(1-\alpha)b]^2}\,, \quad (4.13)$$

and integrate in Eqs. (4.9) and (4.10) over $d\vec{q}$, with the result[18]

$$R_{\pm}^0(t)=\frac{\pi}{m^3}\sigma_{\pm}L^0\sigma\,, \quad (4.14)$$

$$R^1(t)=-\frac{\pi}{m^3}\epsilon L^1\sigma\,, \quad (4.15)$$

where

$$L^0(\sigma)=\frac{\sinh\pi\alpha_s}{\pi\alpha_s}\int_0^1\int d\alpha\,d\beta\,\frac{\alpha^{-\gamma}(1-\alpha)^{\gamma}(1-2\alpha)\beta^2}{[\beta\sigma^2F+1-\beta]^2} \quad (4.16)$$

$$L^1(\sigma)=\frac{\sinh\pi\alpha_s}{\pi\alpha_s}\int_0^1\int d\alpha\,d\beta\,\frac{\alpha^{-\gamma}(1-\alpha)^{\gamma}\beta(1-\beta)}{[\beta\sigma^2F+1-\beta]^2} \quad (4.17)$$

and the functions

$$F\equiv 1-(1-2\alpha)^2\beta\,,$$
$$\sigma\equiv\frac{|\vec{u}|}{m}\,,\quad \sigma_{\pm}\equiv\frac{u_x\pm iu_y}{m}\,,\quad \gamma\equiv i\alpha_s\,, \quad (4.18)$$
$$\epsilon\equiv\frac{1-\sigma^2}{1+\sigma^2}$$

have been introduced. Straightforward application of the Mellin-transformation techniques permits evaluation of the σ behavior for small values. The result, after a lengthy but straightforward calculation, is[18]

$$L^0=\frac{i}{2\alpha_s}\frac{1}{\sigma^2}\left(\frac{1}{1+\sigma^2}\right) +4\gamma[\mathrm{Re}\psi(1+\gamma)-\psi(1)+\tfrac{1}{2}\ln 4]+\cdots, \quad (4.19)$$

$$L^1=-\left(\frac{1}{1-\sigma^2}\right)^2\ln\left(\frac{2\sigma}{1+\sigma^2}\right)^2+\cdots. \quad (4.20)$$

In evaluating Eqs. (4.16) and (4.17) we have limited ourselves to the most singular terms which correspond to $1,3,\ldots$ gluon exchange for L^0 and to $2,4,\ldots$ gluon exchange for L^1. This is consistent with C invariance, which requires that an even number of gluons be exchanged for orthocharmonium and an odd number for parachar-monium. Since color conservation forbids single-gluon exchange, the first contribution to L^0 in Eq. (4.19) has to be dropped. It represents the Born approximation and would be analogous to Primakoff photoproduction of η_c. L^0 and L^1 can be expressed in closed form as derived in Ref. 21 and also recently discussed in Ref. 22:

$$L^0=\xi^0\frac{V(\epsilon^2)}{V1}\,,\quad L^1=\xi^1\frac{W(\epsilon^2)}{V(1)}\frac{\epsilon^2}{\ln(1-\epsilon^2)}\,, \quad (4.21)$$

where

$$\xi^0\equiv\frac{i}{2\alpha_s}\frac{1}{\sigma^2}\left(\frac{1}{1+\sigma^2}\right),\quad \xi^1\equiv-\left(\frac{1}{1-\sigma^2}\right)^2\ln\left(\frac{2\sigma}{1+\sigma^2}\right)^2, \quad (4.22)$$

and

$$V(\epsilon^2)\equiv{}_2F_1(-\gamma,\gamma,1;\epsilon^2)\,,\quad W(\epsilon)\equiv{}_2F_1(1-\gamma,1+\gamma,2;\epsilon^2)\,. \quad (4.23)$$

The above derivation is based upon the fact that the binding effect of the produced parton pair may be ignored, and thus essentially we determined the production of two free c quarks which move with the same momentum. Before going to the numerical evaluation and phenomenological discussion of this model we indicate a possible extension of this formalism which accounts for the binding effects. We return to Eq. (3.13) and write it in the form

$$T_{\lambda\lambda'}=\int_{-\infty}^{+\infty}\frac{d\vec{q}}{(2\pi)^2}\,\xi(\vec{q},\vec{u})J_{\lambda\lambda'}(\vec{q},\vec{u})\,, \quad (4.24$$

where $\xi(\vec{q},\vec{u})$ is defined in Eq. (3.13) and $J_{\lambda\lambda'}$ for specific helicities may be given by

$$J(\vec{q},\vec{u})\equiv\int_{-1/2}^{+1/2}d\beta\int\frac{d\vec{l}}{(2\pi)^2}\frac{(l_{\perp})}{m^2+\vec{l}^2} \times\phi(\vec{L},M_B\beta)|_{\vec{L}=\vec{k}+\vec{q}-2\beta\vec{u}}\,. \quad (4.25)$$

Using the Fourier-transformed bound-state wave function

$$\Phi(\vec{L})=\int_{-\infty}^{+\infty}\frac{d\vec{r}}{(2\pi)^3}\,e^{i\vec{L}\cdot\vec{r}}\phi(\vec{r})\,, \quad (4.26)$$

we may rewrite Eq. (4.24) in the factorized form

$$T=\int_{-\infty}^{+\infty}\frac{d\vec{r}}{(2\pi)^2}\,I_1(\vec{r},\vec{u})I_2(\vec{r})I_3(\vec{r},\vec{u})\,, \quad (4.27$$

where I_1 stands for the interaction between the quarks and the exchanged gluons, I_2 describes the quark-creation process, and I_3 parametrizes the bound-state nature of the quark-antiquark system. The explicit forms are

$$I_1(\vec{r},\vec{u})\equiv\int_{-\infty}^{+\infty}d\vec{q}e^{i\vec{q}\cdot\vec{r}}\xi(\vec{q},\vec{u})\,, \quad (4.28)$$

$$I_2(\vec{r}) \equiv \int_{-\infty}^{+\infty} d\vec{l} e^{i\vec{l}\cdot\vec{r}} \frac{(l_+)}{m^2+\vec{l}^2}, \tag{4.29}$$

$$I_3(\vec{r},\vec{u}) \equiv \int_{-\infty}^{+\infty} \frac{d\gamma_3}{(2\pi)} \int_{-1/2}^{+1/2} d\beta e^{-i\beta(2\vec{u}\cdot\vec{r}-M_B\gamma_3)} \phi(\vec{r}). \tag{4.30}$$

Further simplification of these expressions is involved. Since our main interest in this paper is in the effects due to gluons, we leave the nature of bound-state corrections for a later investigation.

V. NUMERICAL RESULTS

The numerical evaluation of this model is straightforward. Before presenting the results let us first make a few observations about the formulas.

We first consider $c\bar{c}$ photoproduction in an ortho state like $\rho, \omega, \ldots, \psi, \ldots$. The amplitude $R^1(t)$ has a universal zero at $\sigma = 1$ corresponding to $\sqrt{-t} = 2m$ due to the logarithmic term in $L^1(\sigma)$. (This apparent divergence cancels out the zero in ϵ.) This zero is already present in the two-gluon-exchange term. Its position in the momentum-transfer variable depends upon the mass of the constituents m; thus, if a heavy-quark system is produced, the minimum lies far out in $-t$, whereas a light-quark system has the minimum at lower t values.

Plotting $-t/4m_c^2$ should then reveal a constant and fixed minimum point at +1. We now consider photoproduction of the para $c\bar{c}$ state. Keeping only the first term in L^0, we find the Born amplitude of single-gluon exchange, which, however, is forbidden by color conservation. It shows an angular distribution with a sharp spike in the forward direction, like $1/t$, which then falls to zero. Both amplitudes R^0 and R^1 depend only on the variable σ, and therefore scale in the quark mass if a change in the overall size of the cross section is ignored. Since we are working in the infinite-momentum frame, the dependence on the initial energy $E_{\text{c.m.}}$ has completely dropped out; our formalism is therefore not valid in the threshold region and is preferentially applied in the asymptotic region where the diffraction phenomena seem to dominate. The bound-state wave function $\phi_0(\alpha_s, m_c)$ most likely depends on the mass of the quarks as well as the strong-coupling constant. This dependence is undefined unless a specific choice of the bound-state wave function is made. As an attempt we assume the form resulting from a Coulomb potential

$$\phi_0 = \frac{1}{(\pi a_0^3)^{1/2}}, \quad a_0 \equiv \frac{2}{m_c \alpha_s}, \quad \alpha_s \equiv \frac{g_s^2}{4\pi}. \tag{5.1}$$

Ignoring the mass dependence of the bound-state wave function ϕ_0, both amplitudes R^0 and R^1 are proportional to $m_c^{-7/2}$. Note that the above results show no dependence on the target (nucleon) size since we have used an infinitely extended $1/r$ gluon potential.

We have numerically evaluated the shape of the differential cross section for ψ_c photoproduction, adjusting the bound-state wave function at the origin ϕ_0 in Eq. (5.1) by a multiplicative factor such that its size agrees with the data at $E_{\text{c.m.}} \sim 120$ GeV. In Fig. 3(a) we show its shape for $m_c = 1.5$ GeV and $\alpha_s = 0.5$; the analogous curves in

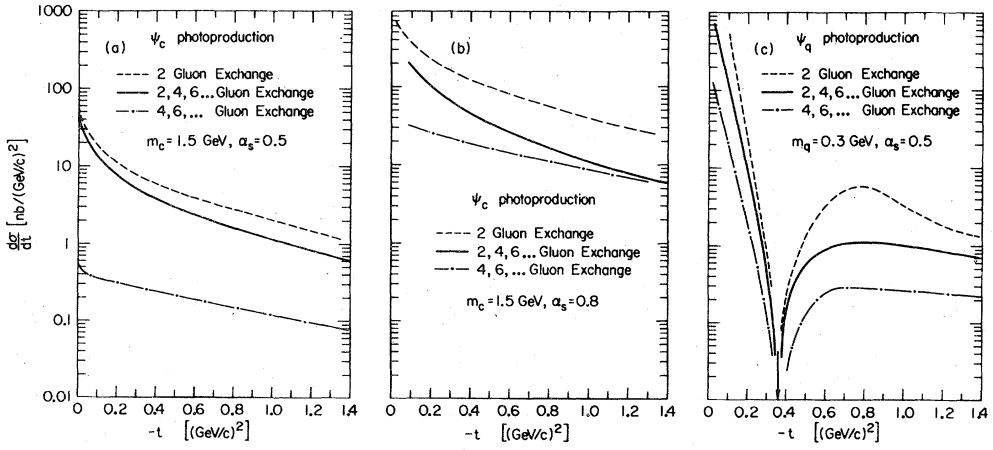

FIG. 3. (a) and (b) Photoproduction of orthocharmonium (ψ_c). The solid line represents 2, 4, 6... gluon exchange, the dashed line indicates the importance of 2-gluon exchange alone, whereas the dashed-dotted line shows the cross-section size of 4, 6...gluon exchange. The parameters are $m_c = 1.5$ GeV and $\alpha_s = 0.5$, and $\alpha_s = 0.8$. (c) Photoproduction of an ortho $q\bar{q}$ state (ψ_q). The solid line, dashed line and dashed-dotted line represent 2, 4, 6, ... gluon exchange. The parameters are $m_q = 0.3$ GeV and $\alpha_s = 0.5$.

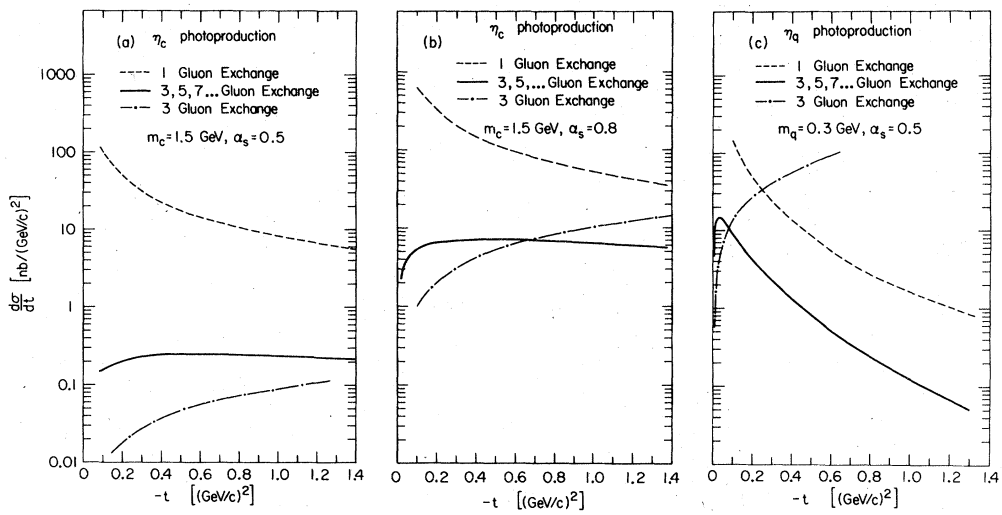

FIG. 4. (a) and (b) Photoproduction of paracharmonium (η_c). The solid line represents 3, 5, 7, ... gluon exchange, the dashed line indicates single-gluon exchange (which is forbidden by color conservation), and the dotted line indicates the size of the 3-gluon exchange near the forward direction. The parameters are $m_c = 1.5$ GeV, $\alpha_s = 0.5$, and $\alpha_s = 0.8$. (c) Photoproduction of a para $q\bar{q}$ state (η_q). The solid line, dashed line, and dotted line represent 3, 5, 7,... gluon exchange, single-gluon exchange and 3-gluon exchange. The parameters are $m_q = 0.3$ GeV and $\alpha_s = 0.5$.

Fig. 3(c) are for $m_q = 0.3$ GeV. The dashed lines (2-gluon exchange) represent the lowest-order contribution. The solid lines (2, 4, 6, ... gluon exchanges) take multigluon corrections into account, and the dashed-dotted lines (4, 6, ... gluon exchanges) have the 2-gluon exchange subtracted. One notices that the 2-gluon-exchange approximation is damped down by the higher-order multigluon exchanges, which, however, interfere such that their contribution is about one order of magnitude smaller. An exponential fit in the region $0.1 \leq -t \leq 0.6$ (GeV/c)^2 gives a slope parameter $b \sim 2$–4 GeV^{-2}; it is less for 4, 6, ... gluon exchange. Mass extrapolation to $m_q = 0.3$ GeV [Fig. 3(c)] brings the zero point in the amplitude R^1 [see Eq. (4.10)] to $-t = 0.36$ (GeV/c)^2. This diffraction minimum is not observed in ρ photoproduction,[23] and it might disappear if the relativistic bound-state nature of the ρ meson is taken into account.

In Figs. 4(a) and 4(c) we show the analogous curves for photoproduction of the para states η_c and η_q. For illustrative purpose we have drawn the Born approximation (which, however, is forbidden by color conservation); it is strongly peaked for small $|t|$ values. 3, 5, ... gluon exchange is flat over a long t range and bends off towards zero in the extreme forward direction. The same calculation with $m_c = 0.3$ GeV shows a rising curve towards smaller $|t|$ values with $b \sim 5$ GeV^{-2} and a decrease to zero in the extreme forward direction.

In Figs. 3(b) and 4(b) the value of the strong-coupling constant is changed to $\alpha_s = 0.8$, but the quark mass is kept at $m_c = 1.5$ GeV. Comparing Figs. 3(a) and 3(b) one notices that the curves rise by a factor of 5 – 10 in going from $\alpha_s = 0.5$ to 0.8. Furthermore, the sum of terms describing 4, 6, ... gluon exchange is much more influential relative to the 2-gluon-exchange term. The fact that at larger $(-t)$ values the 4, 6, ... gluon exchange and the 2, 4, 6, ... gluon exchange contributions are of similar size is a consequence of the interference pattern between the amplitudes T_2 and T_{46}...; however, the qualitative shape of the curves changes little. Similar conclusions can be drawn by comparing the diagrams in Figs. 4(a) and 4(b). Again one finds that the relative size of the various contributions becomes narrower. Note in particular that the 3-gluon exchange is of almost equal size as the cross section due to 3, 5, ... gluon exchange. The trend we see here is that the influence of the multigluon exchange terms is more strongly felt as we increase the coupling strength of the gluonic interaction. It is in agreement with the intuitive expectation that higher-order terms become more strongly felt.

So far we have not mentioned the application of the above formalism to the production of a particle system which interacts predominantly by electromagnetic force. Primakoff photoproduction of an unbound $\tau^+\tau^-$ system (τ^+ and τ^- produced with equal momenta) in the multiple charged field of nuclei is an example. The replacement of the exchanged-gluon coupling constant $\alpha_s \to Z\alpha$ ($\alpha \equiv e^2/4\pi$, $Z \equiv$ nucleus charge) and explicit calculation show that the higher-order corrections

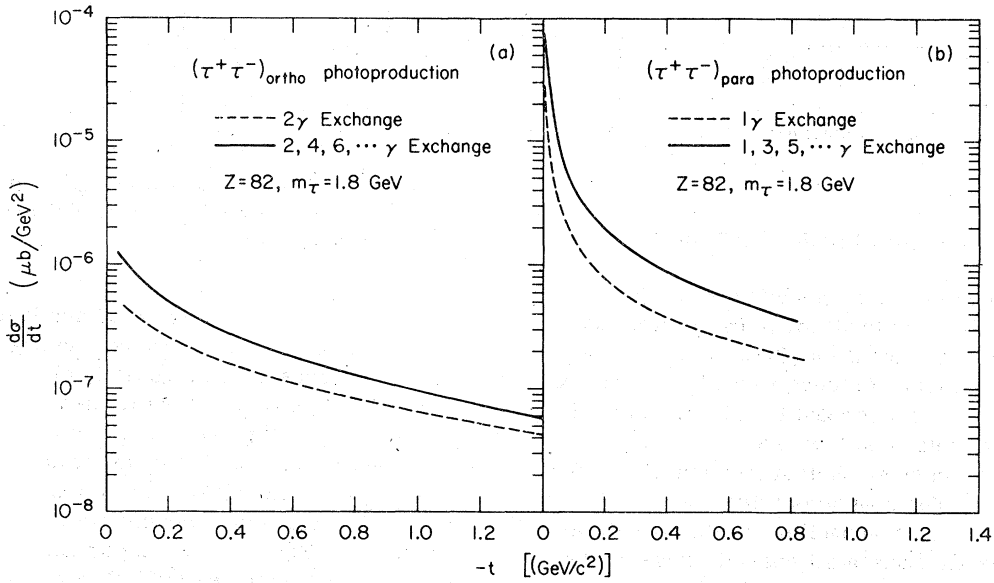

FIG. 5. (a) and (b) Photoproduction of a $\tau^+\tau^-$ pair in an (a) ortho and (b) para state. The solid line in (a) (in (b)) represents 2, 4, 6,... (1, 3, 5,...) photon exchange, whereas the dashed line indicates the size of 2 photon (1 photon) exchange. The nucleus charge is chosen to be $Z=82$ and $m_\tau = 1.8$ GeV.

are nonnegligible and in fact enhance the cross section by a factor of 2–3.

The production of the unbound $\tau^+\tau^-$ para state in the single-photon approximation leads to the familiar form

$$\left(\frac{d\sigma}{dt}\right)_{\text{para}} = 8\pi\alpha^4(\alpha Z)^2 \frac{m_\tau^2}{t}\left(\frac{1}{t-4m_\tau^2}\right)^2, \quad (5.2)$$

which gives the integrated cross section

$$\sigma_{\text{para}} \simeq \frac{\pi}{m_\tau^2}\alpha^4(\alpha Z)^2 \ln\frac{E_{\text{lab}}}{m_e}. \quad (5.3)$$

The differential distribution and integrated cross section for production of the analogous $\tau^+\tau^-$ ortho state are not as suppressed as they might seem by considering the extra factor α^2 (due to the exchange of the additional photon), since the electromagnetic field of the nucleus contributes an additional factor Z. In Fig. 5 we show the shapes and sizes of the differential cross sections. We emphasize that these results may not be applied to "leptonium" photoproduction[15] since we have ignored the electromagnetic binding forces. Since these are very weak, the resulting t-dependent form factor is exponentially damped with a large slope value, so that the integrated cross sections are orders of magnitude below the ones given in Fig. 5.

VI. OTHER DIAGRAMS

In the above analysis we have considered a specific class of gluon-exchange diagrams for the description of the interactions between the photoproduced heavy-quark pair and the nucleon. Quantum chromodynamics, however, does permit a much larger class of diagrams which has been ignored so far. In this section we attempt an estimate of the importance and influence of these diagrams. Primarily we wish to know whether the class of diagrams with multigluon couplings as shown in Fig. 6 can be neglected.

To simplify the discussion we ignore any interaction among the two heavy quarks and draw the diagrams with the two quarks leaving in opposite direction (Fig. 7). The class of diagrams con-

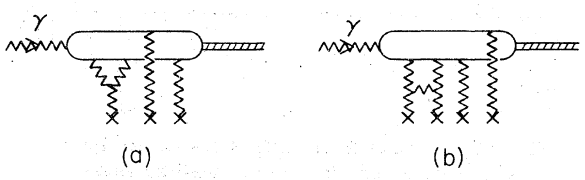

FIG. 6. Gluon tree diagrams which have been ignored in the model.

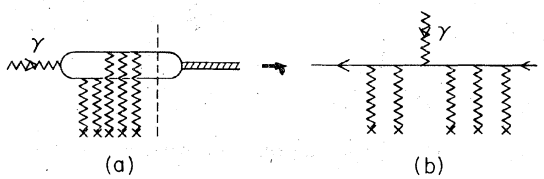

FIG. 7. Cutting and opening of the fermion loop.

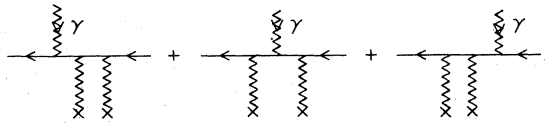

FIG. 8. Ladder-type diagrams of order g_s^4 considered by the model.

tributing to this process is subject to the two constraints:

(i) The number of gluons attached to the c-quark lines must be even (odd) for ψ_c (η_c) photoproduction owing to Furry's theorem (C-parity conservation).

(ii) The number of gluons which are exchanged between the gluon source and the $c\bar{c}$ pair must be ≥ 2 owing to color conservation.

Let us first consider photoproduction of an ortho bound state. The diagrams contributing in lowest order g_s^4 (the gluon-coupling constant), with the gluon lines attached in all possible ways on the quark lines, are indicated in Fig. 8. In next order g_s^6 tree diagrams such as those shown in Fig. 9(a) are excluded, since an uneven number of gluons is attached to the quark lines violating constraint (i). In order g_s^8 the tree diagram which might spoil our earlier results is of the type shown in Fig. 9(b). That these diagrams give contributions which are unimportant is ensured by the following two points:

(a) Since we have carried out all our analysis assuming that perturbation theory is applicable, the gluon coupling has to be smaller than 1; as a consequence, contributions to order g_s^8 are suppressed with respect to order g_s^4.

(b) We have carried out a numerical analysis of the influence of the triangle-loop diagram by comparing the size of the diagrams in Fig. 10.

Our findings are that the amplitude of diagram (b) in Fig. 10 is *suppressed by two orders of magnitude* with respect to the amplitude of diagram (a) in Fig. 10 (we have here not included the additional suppression due to the gluon coupling constant). The influence of the third type of diagrams, also much smaller than diagram (a) in Fig. 10, is absorbed in the gluon vertex renormalization and therefore does not concern us. Adding extra gluon exchanges does not substantially change this picture. As a result we come to the conclusion that, in low orders of g_s, tree diagrams are suppressed with respect to ladder-type diagrams.

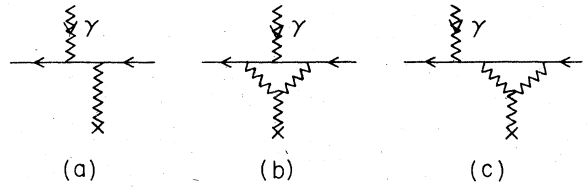

FIG. 10. Estimate of the size of the single-gluon-exchange diagram (a) versus the size of the simplest gluon tree diagram (b), (c).

We now consider photoproduction of the para state. The class of diagrams we have to compare is shown in Fig. 11. The importance of these diagrams is estimated by the following chain of arguments:

(a) Both diagrams are cut along the dashed lines and the size of the remaining amplitudes on the left-hand side will be estimated and compared.

(b) We have mentioned earlier that the size of the triangle-loop diagram [Fig. 10(b)] has been estimated with respect of the single-gluon-exchange diagram [Fig. 10(a)]; it is suppressed by two orders of magnitude in amplitude.

(c) The differential cross section resulting from the diagram in Fig. 10(b) is four orders of magnitude below the single-gluon exchange in Fig. 10(a) which means: $(d\sigma/dt)_{\text{triangle}} \approx 10^{-2}$ nb/GeV^2. The corresponding value for the diagram of Fig. 11(a) (left of dashed line) is determined using Fig. 3(a): $(d\sigma/dt)_{\text{two-gluon}} \approx 1-10$ nb/GeV^2. We thus conclude that the contribution of diagram (a) is substantially more important than diagram (b) (Fig. 11).

Our findings are that tree diagrams contribute in η_c photoproduction in the same order of g_s as ladder-type diagrams. However, their contribution is orders of magnitude below the ladder diagrams considered above. Note that this result does not substantially change if α_s grows or the quark mass is changed.

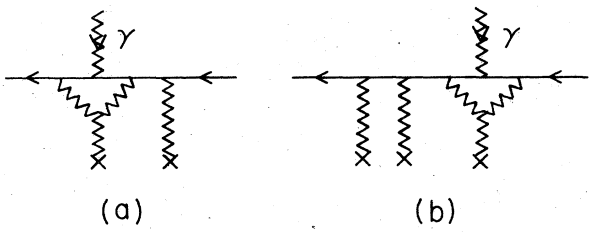

FIG. 9. Gluon tree diagrams of order g_s^6 (a) and order g_s^8 (b).

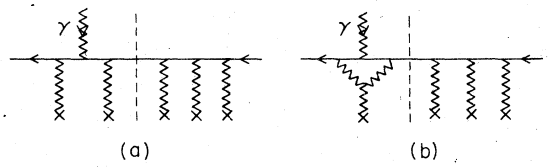

FIG. 11. Estimate of the size of the ladder-type diagrams (a) versus the size of the tree-like gluon exchange diagrams (b), (c).

VII. CONCLUSION

In this paper we have presented an analysis of photoproduction of a heavy-fermion pair, assuming that it interacts via a long-range gluon potential with the target nucleon. Within the framework of the Cheng-Wu picture, a theory has been developed for para and ortho quark-pair production assuming that gluons are responsible for the interaction with the target. The characteristics of the resulting angular distributions have been determined; in particular, the sizes and shapes of 3 and $3,5,\ldots$ gluon exchanges for para production, and 2 and $2,4,\ldots$ gluon exchanges for ortho production were found. The angular distribution for η_c production is predicted to be flat, and the cross section to be in the nanobarn range, whereas it exponentially decreases in the case of ψ_c photoproduction. We also were able to show that diagrams with three or more gluons attached to each other (gluon trees) may safely be neglected. The theory also has been applied to photoproduction of an unbound $\tau^+\tau^-$ pair where multiphoton exchanges were found to enhance the cross sections by a factor of 2–3.

ACKNOWLEDGMENTS

I would like to thank Fred Gilman for his reading of the manuscript and for clarifying discussions, and Peter Lepage for his improvements of the text. Inspiring and clarifying conversations with Peter Lepage, Henry Tye, Hannu Miettinen, Peter Scharbach, Professor C. Schmid, and Professor D. Horn are gratefully acknowledged. This research was partially supported by the U. S. Energy Research and Development Administration.

[1]H. Fritzsch, M. Gell-Mann, and H. Leutwyler, Phys. Lett. 47B, 365 (1973); S. Weinberg, Rev. Mod. Phys. 46, 255 (1974); W. Marciano and H. Pagels, Rockefeller Univ. Report No. COO-2232B-130 (unpublished); B. Humpert (unpublished).

[2]F. E. Low, Phys. Rev. D 12, 163 (1975); S. Nussinov, Phys. Rev. Lett. 34, 1286 (1975); Phys. Rev. D 14, 246 (1976); T. Appelquist and H. D. Politzer, Phys. Rev. Lett. 34, 43 (1975).

[3]S. J. Brodsky and J. E. Gunion, Phys. Rev. Lett. 37, 402 (1976).

[4]S. J. Brodsky, R. Blankenbecler, and J. F. Gunion, Stanford Linerar Accelerator Center Report No. SLAC-PUB-1938 (unpublished).

[5]J. Ellis, M. K. Gaillard, and G. Ross, Nucl. Phys. B111, 253 (1976).

[6]S. D. Drell, Stanford Linear Accelerator Center, Report No. SLAC-PUB-1683, 1975 (unpublished); H. Joos, in *Current Induced Interactions*, proceedings of the Summer School on Theoretical Particle Physics, Hamburg, 1975, edited by J. G. Körner, G. Kramer, and D. Schildknecht (Springer, New York, 1976), p. 428; S. Yankielowicz, Stanford Linear Accelerator Center Report No. SLAC-PUB-1800, 1976 (unpublished).

[7]M. K. Gaillard, B. W. Lee, and J. L. Rosner, Rev. Mod. Phys. 47, 277 (1975).

[8]A. De Rújula, Harvard University report, 1976 (unpublished).

[9]See for example, G. S. Abrams, in *Proceedings of the 1975 International Symposium on Lepton and Photon Interactions at High Energies, Stanford, California*, edited by W. T. Kirk (Stanford Linear Accelerator Center, Stanford, 1976), p. 25; R. Prepost, *ibid.* p. 241. For a review see B. Humpert, *Dynamical Concepts on Scaling Violation and the New Resonances in e^+e^- Annihilation*, Lecture Notes in Physics, No. 45 (Springer, Heidelberg, 1976).

[10]B. Humpert and A. C. D. Wright, Phys. Lett. 65B, 463 (1976); Phys. Rev. D 15, 2503 (1977); Ann. Phys. (N.Y.) 110, 1 (1978).

[11]B. Humpert, Phys. Lett. 68B, 66 (1977).

[12]H. Cheng and T. T. Wu, in *Proceedings of the* 1971 *International Symposium on Electron and Photon Interactions at High Energies*, edited by N. B. Mistry (Laboratory of Nuclear Studies, Cornell University, Ithaca, New York, 1972), p. 147 and Ref. 12.

[13]R. Blankenbecler and R. L. Sugar, Phys. Rev. D 2, 3024 (1970); Phys. Rev. 183, 1387 (1969); S. J. Chang, Univ. of Illinois Report No. ILL-(Th-) 76-13, 1976 (unpublished).

[14]J. D. Bjorken, J. B. Kogut, and D. E. Soper, Phys. Rev. D 3, 1382 (1971); Phys. Rev. D 1, 2901 (1970); S. Brodsky, R. Roskies, and R. Suaya, Phys. Rev. D 8, 4574 (1973). J. Kogut and L. Susskind, Phys. Rep. 8C, 75 (1973).

[15]I. J. Muzinich, E. A. Paschos, and D. P. Sidhu, BNL report, 1976 (unpublished); A. Halprin and H. Primakoff, Phys. Rev. D 14, 1776 (1976); J. W. Moffat, Phys. Rev. Lett. 35, 1605 (1975).

[16]H. D. Politzer, Nucl. Phys. B129, 301 (1977)

[17]H. D. Politzer, Phys. Rep. 14C, 130 (1974).

[18]H. Cheng and T. T. Wu, Phys. Rev. 182, 1873, (1969); Phys. Rev. D 5, 3077 (1972); Phys. Rev. D 6, 2637 (1972).

[19]S. D. Drell, D. J. Levy, and T. M. Yan, Phys. Rev. D 1, 1617 (1972).

[20]L. I. Schiff, *Quantum Mechanics* (McGraw-Hill, New York, 1968).

[21]H. Bethe and L. C. Maximon, Phys. Rev. 93, 768 (1954).

[22]T. Jaroszewicz and J. Wosiek, Munich report (unpublished).

[23]W. Lee, in *Proceedings of the 1975 International Symposium on Lepton and Photon Interactions at High Energies, Stanford, California* (Ref. 9), p. 635.